

Ion heating during reconnection in the Madison Symmetric Torus reversed field pinch^{a)}

S. Gangadhara,^{1,2} D. Craig,^{1,3,b)} D. A. Ennis,^{1,2} D. J. Den Hartog,^{1,2} G. Fiksel,^{1,2}
and S. C. Prager^{1,2}

¹*Center for Magnetic Self-Organization in Laboratory and Astrophysical Plasmas,
Princeton, New Jersey 08542, USA*

²*University of Wisconsin–Madison, Madison, Wisconsin 53706, USA*

³*Wheaton College, Wheaton, Illinois 60187, USA*

(Received 15 November 2007; accepted 30 January 2008; published online 8 May 2008)

Measurements of localized ion heating during magnetic reconnection in the Madison Symmetric Torus reversed field pinch [R. N. Dexter, D. W. Kerst, T. W. Lovell, S. C. Prager, and J. C. Sprott, *Fusion Technol.* **19**, 131 (1991)] are presented using two beam-based diagnostics: Charge exchange recombination spectroscopy and Rutherford scattering. Data have been collected from three types of impulsive reconnection event, in which the resistive tearing mode activity associated with reconnection is present either in the edge plasma, the core plasma, or throughout the plasma volume. A drop in the stored magnetic energy is required for ion heating to be observed during magnetic reconnection, and when this occurs, heating is concentrated in regions where reconnection is taking place. The magnitude of the observed temperature rise during reconnection varies with ion species, suggesting that the heating mechanism has a mass and/or charge dependence. Both the magnitude and spatial structure of the observed temperature rise also depend on the plasma current and density. Nonetheless, the fraction of released magnetic energy converted to ion thermal energy remains roughly constant over a range of plasma conditions. © 2008 American Institute of Physics.

[DOI: [10.1063/1.2884038](https://doi.org/10.1063/1.2884038)]

I. INTRODUCTION

Magnetic reconnection is a process by which the magnetic topology of a plasma is changed through the tearing and reconnecting of magnetic field lines. During this process, plasma ions are often energized through the conversion of magnetic energy into thermal energy. As a result, ion heating is often observed to accompany magnetic reconnection in both laboratory and astrophysical plasmas. Ion heating associated with magnetohydrodynamic (MHD) fluctuation activity and magnetic reconnection has been observed in a number of laboratory experiments—such as in the tokamak,¹ the reversed field pinch (RFP),^{2–6} the spheromak,^{7,8} and the spherical tokamak^{9,10}—as well as in the solar corona^{11,12} and in the Earth's magnetosphere.¹³ In many cases, magnetic reconnection and the associated heating occur impulsively in the form of a sudden event following a long quiescent period during which the plasma evolves slowly. In astrophysical plasmas, impulsive reconnection occurs during solar flares¹⁴ and magnetospheric substorms,¹⁵ while in the lab it occurs during sawtooth crashes in the tokamak¹⁶ and RFP.¹⁷

Although ion heating is often observed during magnetic reconnection, the means by which energy is transferred from the magnetic field to the ions is unknown. In order to gain insight into possible heating mechanisms, the relationship between the spatial distribution of the ion heating and the spatial location of reconnection must be understood. This

relationship has been explored in some low-temperature plasma experiments.^{18,19} However, this relationship has been difficult to investigate in most high-temperature fusion plasmas, as measurements of ion heating during reconnection in these devices are generally line-of-sight. Such line-of-sight measurements provide only the line-averaged response of ions to reconnection. Understanding this response is further complicated by the fact that in many cases, localized reconnection takes place simultaneously at multiple sites throughout the plasma volume. Thus, localized measurements of ion heating are required to directly determine the relationship between heating and reconnection.

In this paper, localized measurements of the ion temperature evolution during impulsive reconnection in the Madison Symmetric Torus (MST) RFP²⁰ will be described. In Sec. II, a brief description of MST and of the diagnostics used to measure ion temperature will be provided. The three types of impulsive reconnection event during which ion temperature has been measured will be described in Sec. III, while results for the temperature evolution during each of these types of reconnection event will be presented in Sec. IV. During the first type of event, reconnection is limited to the edge; the drop in stored magnetic energy is modest, and ion heating is limited to the outer half of the plasma. In the second kind of event, many coupled reconnection sites exist throughout the plasma, the drop in stored magnetic energy is larger, and ion heating occurs at all radii. In both cases, the ion temperature rise occurs on a fast time scale, of order the reconnection time, and in both cases the drop in magnetic energy is sufficient to explain the observed rise in ion temperature. In the third type of reconnection event, reconnection

^{a)}Paper N12 1, *Bull. Am. Phys. Soc.* **52**, 189 (2007).

^{b)}Invited speaker.

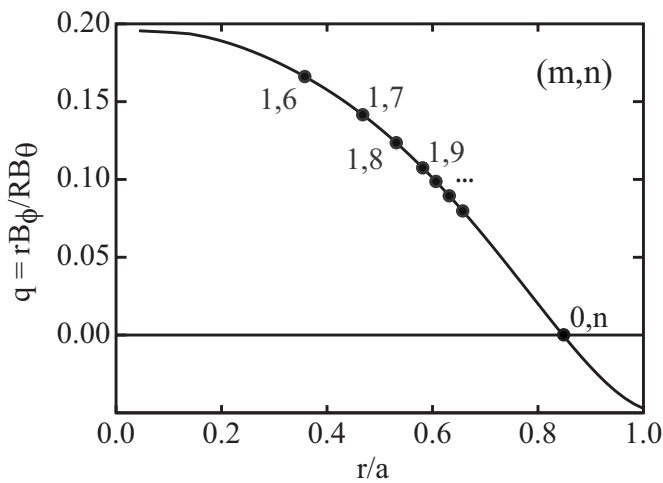


FIG. 1. $q (=rB_\phi/RB_\theta)$ profile for a typical MST discharge at $I_p=400$ kA, $n_e=10^{19}$ m $^{-3}$.

tion is limited to the core, the stored magnetic energy remains approximately constant, and no ion heating is observed at any radial location. The results suggest that a drop in magnetic energy is required for ions to be heated during reconnection, and that when this occurs heating is concentrated near the reconnection layer. Consequently, the large-scale heating observed during a global reconnection event arises from the presence of many heating layers distributed throughout the plasma volume. Results indicate that during such an event, both the radial structure and absolute value of the ion temperature depend strongly on plasma current and density, as described in Sec. V. Results presented in this section also show that the temperature obtained during a global reconnection event depends on ion species, suggesting that heating may be mass- or charge-dependent. Several theoretical models have been advanced to explain the observed heating, although none has emerged as clearly superior. A summary of these models and their relationship to the current observations is provided in Sec. VI. Finally, a summary of the main results is presented in Sec. VII.

II. ION HEATING MEASUREMENTS IN MST

A plot of the $q (=rB_\phi/RB_\theta)$ profile for a typical MST discharge is shown in Fig. 1. Within this magnetic topology, there are many rational surfaces where reconnection can take place. Reconnection in MST is usually driven by the presence of current-driven resistive tearing modes,²¹ and in Fig. 1 circles have been placed on top of the q profile to indicate the location of resonance for the modes with the largest amplitude. In the plasma core, the dominant modes have a poloidal mode number of $m=1$ and toroidal mode numbers of $n \approx 6-9$, while the edge plasma is dominated by the $m=0$, $n=1$ mode, which is resonant at the reversal surface where the toroidal magnetic field $B_\phi=0$.

Measurements of the ion temperature during reconnection are obtained on MST using two diagnostics: Charge exchange recombination spectroscopy (CHERS) and Rutherford scattering.²² CHERS is a commonly employed technique in fusion devices for measuring impurity ion

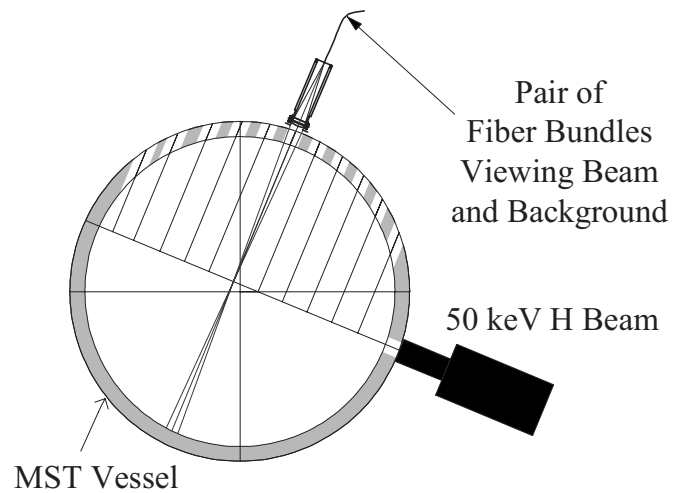


FIG. 2. Cross section of MST, showing the location of the CHERS diagnostic neutral beam and the viewports available for measurements (indicated by parallel lines).

temperature.^{23,24} On MST, a CHERS system has been developed to measure the C^{+6} ion temperature (T_C) with both fast time resolution (10–100 μ s) and good spatial resolution (≈ 2 cm). This temperature is obtained from measurements of C VI emission ($\lambda=343.4$ nm) stimulated by charge exchange between C^{+6} ions and energetic hydrogen atoms injected radially into the plasma via a diagnostic neutral beam. Emission is collected using two fiber bundles (to allow for dynamic background subtraction), which, for a given plasma discharge, are placed on a single viewport, providing measurements from a single radial location. The collected light is dispersed and recorded in a custom-built, high-throughput spectrometer.²⁵ A cross section of MST showing the location of the beam and the viewports available for measurements is given in Fig. 2. Local values for T_C are determined from nonlinear fits to the emission data, in which the carbon ions are assumed to have a Maxwellian distribution, and effects of spin-orbit coupling are included in the model.²⁶

Rutherford scattering (RS) is also a beam-based diagnostic. In this case, the beam is composed of helium atoms, which are injected from the bottom of MST as shown in Fig. 3. The injected atoms undergo scattering primarily as a result of collisions with background deuterium (i.e., majority species) ions. By measuring the energy spectrum of the scattered atoms, the temperature of the scattering agents can be determined, assuming that the D^+ ions follow a Maxwellian distribution.²⁷ Thus, Rutherford scattering provides measurements of the bulk ion temperature (T_B). It is one of the few diagnostics that is able to do so in high-temperature plasmas, and MST is one of the few fusion devices that currently employs such a diagnostic. RS operates with a temporal resolution (10 μ s) that is similar to CHERS. However, the spatial resolution of the RS measurements (≈ 15 cm) is much coarser than for CHERS, and typically measurements are only available from one radial location (although more recently RS data have been obtained at three radial locations). Thus, CHERS is predominantly used to measure the radial structure of the ion temperature evolution during reconnection.

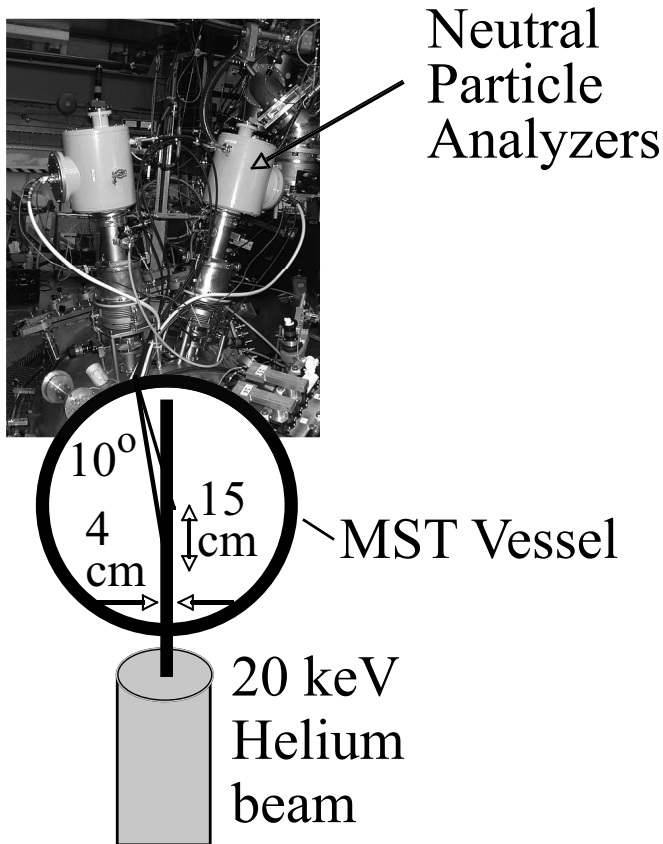


FIG. 3. Cross section of MST, showing the location of the Rutherford scattering beam and the neutral particle energy analyzer.

tion (Secs. IV and V B), with RS measurements providing a comparison between impurity and bulk ion heating during reconnection (Sec. V A).

III. TYPES OF RECONNECTION IN MST

As described above, there are two “types” of tearing modes that drive impulsive reconnection in MST: $m=1$ modes in the plasma core and $m=0$ modes in the plasma edge. As a result, there are three types of impulsive reconnection event that are observed in MST. During a **global reconnection event** (i.e., “sawtooth crash”), linearly unstable $m=1$ modes are excited first, as shown in Fig. 4(b).²⁸ These modes then nonlinearly couple to excite the edge-resonant $m=0$ modes. Once the $m=0$ modes are active, they serve to mediate reconnection activity at the various $m=1$ resonant surfaces, again as a result of nonlinear interaction. Thus, during a global reconnection event, reconnection takes place at many coupled sites throughout the plasma volume. This leads to a significant drop in the plasma stored magnetic energy (~ 15 kJ), as seen in Fig. 4(d).

Global reconnection events are observed in so-called standard plasmas, which contain significant gradients in the plasma current density profile and large fluctuation levels. During enhanced confinement operation, gradients are significantly relaxed and fluctuation activity is reduced. However, edge gradients can develop in such plasmas, leading to instability of the edge-resonant $m=0$ modes. It is under such

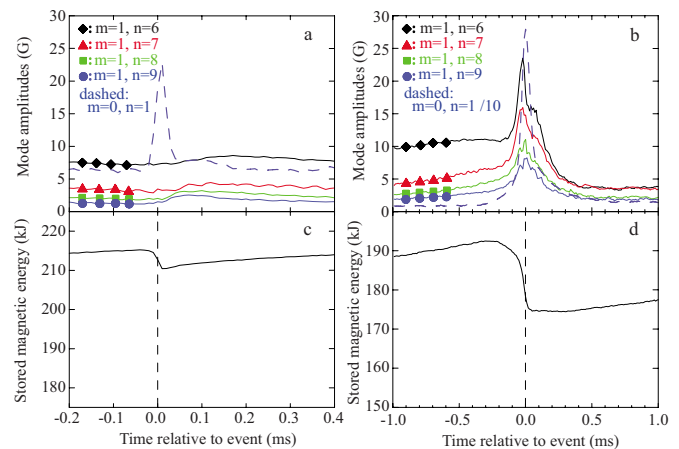


FIG. 4. (Color online) Resistive tearing mode amplitudes [(a), (b)] and stored magnetic energy [(c), (d)] for an edge and global reconnection event. Note that the $m=0, n=1$ tearing mode amplitude is divided by 10 in the plot for the global reconnection event (b). Reprinted with permission from Fig. 1 of S. Gangadhara, D. Craig, D. A. Ennis, D. J. Den Hartog, G. Fiksel, and S. C. Prager, Phys. Rev. Lett. **98**, 075001 (2007). Copyright (2007) by the American Physical Society.

conditions that an **edge reconnection event** is observed.^{29,30} Although $m=0$ modes are excited during such an event, the $m=1$ mode amplitudes remain small, as illustrated in Fig. 4(a). Thus, reconnection is limited to the edge during an edge reconnection event. The increase in the $m=0$ mode amplitude during an edge reconnection event is a factor of ~ 10 smaller than for a global reconnection event. The change in stored magnetic energy [Fig. 4(c)] is correspondingly smaller as well.

Standard plasmas may also be generated during which there is no reversal of the toroidal magnetic field (i.e., $B_\phi > 0$ everywhere in the plasma). In such plasmas there is no $m=0$ resonant surface, and thus no $m=0$ reconnection. For these cases, impulsive reconnection is observed in the form of a **core reconnection event**. An example of such an event is shown in Fig. 5. Both the temporal behavior and the amplitudes of the core-resonant $m=1$ modes during a core reconnection event [Fig. 5(a)] are similar to that in a global reconnection event [Fig. 4(a)]. Conversely, the $m=0$ mode amplitude remains at a low level during the event, as expected. Surprisingly, there is also no change in the stored magnetic energy during a core reconnection event, as seen in Fig. 5(b). This result suggests that the amount of magnetic energy released during reconnection depends strongly on the presence of the $m=0$ modes.

IV. MEASUREMENTS OF ION HEATING DURING IMPULSIVE RECONNECTION

The C^{+6} ion temperature evolution has been measured for the three types of reconnection event described in Sec. III using CHERS. Results for a **global reconnection event** are shown in Fig. 6, for data obtained at five radial locations (ranging from $r/a=0$ to 0.75). The results represent an ensemble-average over a number of similar events, for plasma conditions of $I_p=390$ kA and $n_e=10^{19}$ m⁻³. Error bars were determined by assuming the signal noise to be

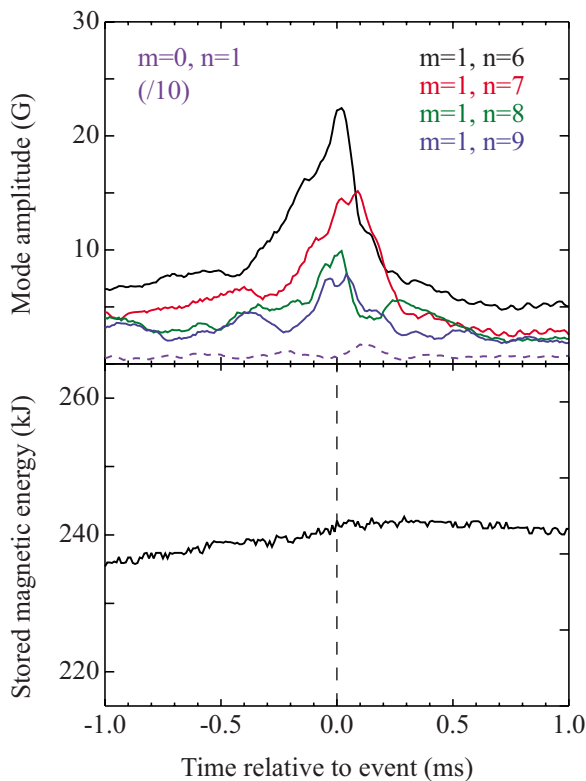


FIG. 5. (Color online) Resistive tearing mode amplitudes (top) and stored magnetic energy (bottom) for a core reconnection event. Note that the $m=0, n=1$ tearing mode amplitude is divided by 10. Top figure reprinted with permission from Fig. 5a of S. Gangadhara, D. Craig, D. A. Ennis, D. J. Den Hartog, G. Fiksel, and S. C. Prager, Phys. Rev. Lett. **98**, 075001 (2007). Copyright (2007) by the American Physical Society.

dominated by Poisson photon counting statistics.²⁶ Prior to a global reconnection event, the temperature profile is slightly peaked. During the event, the temperature is observed to increase at all measured locations, indicating that ion heating is **global** during a global reconnection event. The temperature increase occurs on a fast time scale ($\sim 200 \mu\text{s}$), of order the reconnection time. The largest values of T_C are observed slightly after the event. This result is consistent with stron-

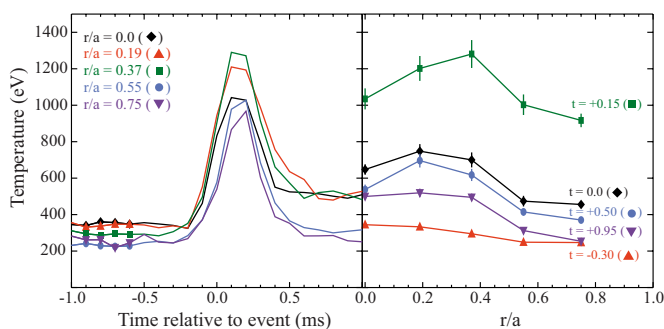


FIG. 6. (Color online) CHERS measurements of ion heating during a global reconnection event. Left: Ensemble-averaged C^{+6} temperature data from five radial locations, for $I_p=390$ kA and $n_e=10^{19} \text{ m}^{-3}$. Right: Radial profile measurements constructed from the temporal data, with each point representing a $100 \mu\text{s}$ average. Reprinted with permission from Fig. 4 of S. Gangadhara, D. Craig, D. A. Ennis, D. J. Den Hartog, G. Fiksel, and S. C. Prager, Phys. Rev. Lett. **98**, 075001 (2007). Copyright (2007) by the American Physical Society.

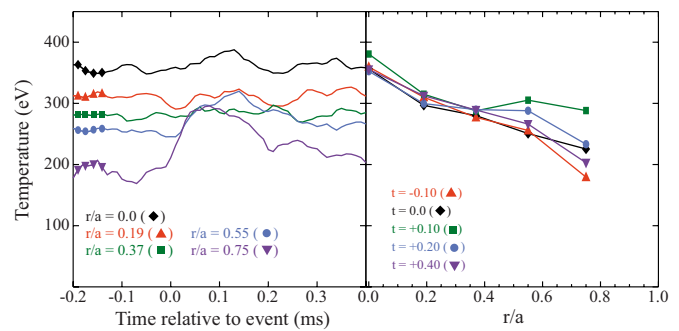


FIG. 7. (Color online) CHERS measurements of ion heating during an edge reconnection event. Left: Ensemble-averaged C^{+6} temperature data from five radial locations, for $I_p=420$ kA and $n_e=0.7 \times 10^{19} \text{ m}^{-3}$. Right: Radial profile measurements constructed from the temporal data, with each point representing a $50 \mu\text{s}$ average. Reprinted with permission from Fig. 3 of S. Gangadhara, D. Craig, D. A. Ennis, D. J. Den Hartog, G. Fiksel, and S. C. Prager, Phys. Rev. Lett. **98**, 075001 (2007). Copyright (2007) by the American Physical Society.

gest heating (=largest dT/dt) during the peak of the event ($t=0$). The largest values for T_C are also observed off-axis, producing a hollow temperature profile. This is consistent with the resonant locations for the dominant $m=1$ tearing modes being off-axis (see Fig. 1). This result suggests that the heating is largest in regions of maximum reconnection.

Results for the temporal evolution of T_C during an **edge reconnection event** are shown in Fig. 7. Data were taken at five radial locations ($r/a=0$ to 0.75), and the results represent ensemble averages taken over a number of similar events, for plasma conditions of $I_p=420$ kA and $n_e=0.7 \times 10^{19} \text{ m}^{-3}$. Error bars were determined by assuming the signal noise to be dominated by Poisson photon counting statistics. Prior to an edge reconnection event, the temperature profile is slightly peaked. During the event, the temperature is first observed to increase at the outermost measurement location, which is the one closest to the $m=0$ resonant surface (at $r/a \sim 0.8$ in these plasmas). Heating at this location occurs on a fast time scale ($\sim 50 \mu\text{s}$), of order the reconnection time. The temperature increase then propagates inward toward $r/a=0.55$. However, the temperature inside of this radius is unaffected, producing a slightly hollow shape to the T_C profile in the core. These results indicate that heating is **limited to the edge** during an edge reconnection event. Heating is strongest at the measurement location closest to the $m=0$ resonant surface, and the largest values for the edge ($r/a > 0.5$) temperature are observed slightly after the crash. Both of these results are similar to those observed during a global reconnection event, and they imply that heating is again largest in regions of maximum reconnection—or in this case, the only region of reconnection.

The results described above indicate that during magnetic reconnection, heating is localized to the reconnection layer, and that the global heating observed during a global reconnection event arises from the presence of multiple reconnection sites distributed throughout the plasma volume. However, not all reconnection events lead to ion heating. The temporal evolution of T_C during a **core reconnection event** is shown in Fig. 8, for data taken at $r/a=0$ and for plasma

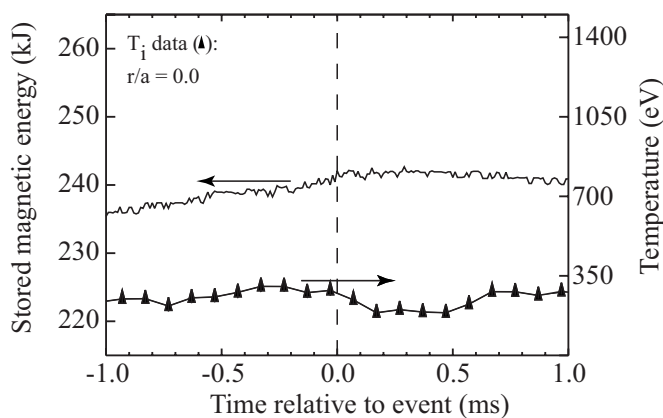


FIG. 8. C^{+6} temperature (bottom line) and stored magnetic energy (top line) for a single core reconnection event. Reprinted with permission from Fig. 5b of S. Gangadhara, D. Craig, D. A. Ennis, D. J. Den Hartog, G. Fiksel, and S. C. Prager, *Phys. Rev. Lett.* **98**, 075001 (2007). Copyright (2007) by the American Physical Society.

conditions of $I_p=400$ kA and $n_e=10^{19}$ m $^{-3}$. These measurements represent data from a single event, during which no significant change to T_C is observed. Similar results have been obtained at four other radial locations ($r/a=0.19$ to 0.75), indicating that there is *no ion heating* during a core reconnection event. While perhaps surprising, the absence of ion heating during a core reconnection event is consistent with the stored magnetic energy remaining constant during such an event (see Fig. 5), indicating that energy from the magnetic field is indeed the source for ion heating during magnetic reconnection. When this energy source is available (as for a global or edge reconnection event), heating is then localized near the reconnection layer. Taken together, these results provide the strongest evidence to date of a direct connection between ion heating and magnetic reconnection in a high-temperature fusion plasma.

V. PARAMETRIC DEPENDENCIES OF ION HEATING DURING RECONNECTION

The results shown in Secs. III and IV imply that $m=0$ modes must be active in order for energy to be released from the magnetic field during reconnection. This may be due to the role that the $m=0$ modes play in mediating reconnection throughout the plasma volume as a result of nonlinear coupling with $m=1$ modes. The role that $m=0$ modes play in modifying the behavior of fluctuating plasma quantities (e.g., \tilde{J} , \tilde{B} , and \tilde{E}) may also be important for understanding magnetic energy release and subsequent ion heating. Thus, the question of how reconnection depends on tearing mode coupling is very much an active area of research on MST.

In this section, we will present studies conducted to investigate other parametric dependencies of ion heating, specifically focused on heating during a global reconnection event. In Sec. V A the dependence of ion heating on ion species will be discussed, and in Sec. V B the variation of ion heating with plasma density and plasma current will be described.

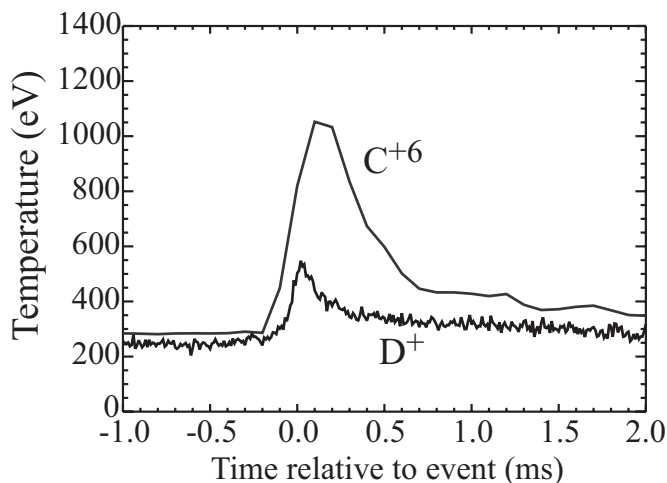


FIG. 9. Ensemble-averaged measurements of the C^{+6} temperature (thin line) from CHERS and the D^+ temperature (thick line) from RS for a global reconnection event. CHERS measurements were obtained at $r/a=0.37$ and RS measurements at $r/a=0.32$.

A. Variation of ion heating with species

As we will see explicitly in Sec. V B, the total amount of energy going into carbon ions during reconnection is a small fraction of the drop in stored magnetic energy. This is primarily because the concentration of C^{+6} ions in the plasma is small. The bulk ion density is of course substantially larger (being a significant fraction of n_e for reasonable values of Z_{eff}), so any significant heating of these ions would correspond to a significant energy gain. Measurements of the bulk ion temperature evolution during a global reconnection event for a single radial location ($r/a=0.32$) using Rutherford scattering are shown in Fig. 9. Also shown in this figure are CHERS measurements of the C^{+6} ion temperature from a similar radial location ($r/a=0.37$). These measurements were both taken in deuterium plasmas. The carbon temperature is observed to be substantially higher than the deuterium temperature during the reconnection event. This result suggests that ion heating during reconnection is stronger for carbon than for deuterium, implying a possible mass or charge dependence to the heating mechanism. However, the observed temperature depends on both heating and confinement. Thus, it may be that heating is similar for both species, while energy confinement is significantly poorer for deuterium ions. For example, charge-exchange losses for the deuterium ions are expected to be significant during reconnection, during which time there is a large influx of neutrals from the wall as a result of the strong plasma-wall interaction. Such losses may act to suppress the deuterium ion temperature relative to the carbon temperature. Other loss mechanisms may also contribute to the observed discrepancy.

Measurements of the bulk and carbon ion temperature evolution during a global reconnection event have also been obtained in helium plasmas. Those results are shown in Fig. 10, where the He^{+2} temperature (at $r/a=0.32$) has been measured using RS and the C^{+6} temperature (at $r/a=0.37$) has been measured with CHERS. In this case, the temperatures

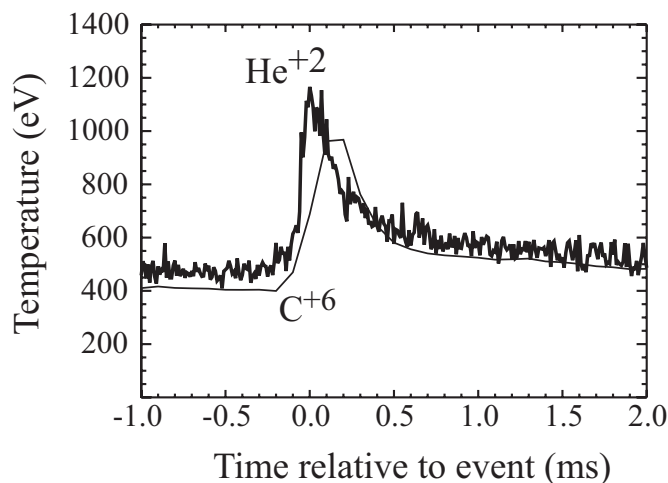


FIG. 10. Ensemble-averaged measurements of the C^{+6} temperature (thin line) from CHERS and the He^{+2} temperature (thick line) from RS for a global reconnection event. CHERS measurements were obtained at $r/a=0.37$ and RS measurements at $r/a=0.32$.

of the two species agree quite well, within the resolution of the measurements. This agreement may simply be the result of similar heating and confinement for the two species (since, for example, charge exchange is not a loss mechanism for He^{+2} ions). However, this agreement may also arise from the balance between a more complicated set of heating and loss mechanisms, which could result in there being a charge or mass dependence to the ion heating during reconnection. Nonetheless, for both deuterium and helium plasmas, there is a significant change in the ion temperature during a global reconnection event, indicating that there is indeed a large energy gain by the ions during reconnection.

The total ion heating power during a global reconnection event is large as well. In Fig. 11, the evolution of the bulk deuterium ion temperature measured with Rutherford scattering at three radial locations is shown during such an event. The data support the conclusion that ion heating is global during a global reconnection event (as initially inferred from the CHERS measurements). In addition, the somewhat stronger edge plasma heating that is observed in the impurity ion temperature profile is reproduced in the bulk T_B profile (compare Figs. 6 and 11). During the event, the bulk ion temperature is observed to increase by about 200 eV over a period of about 100 ms. This implies a heating power of greater than 40 MW being delivered to the ions, which is far greater than the steady Ohmic heating of the electrons during the discharge. The corresponding increase in ion thermal energy is about 4 kJ. The only source of energy capable of providing this heating is the stored magnetic energy, and we have noted above that a change in stored magnetic energy is required for ion heating to be observed during reconnection. The data shown in Fig. 11 were obtained at $I_p=400$ kA and $n_e=10^{19}$ m^{-3} ; for such plasma conditions, the change in magnetic energy is about 20 kJ during a global reconnection event [see Fig. 4(d)]. These results indicate that at least 20% of the magnetic energy loss is transferred to the ions during such an event. If ion energy loss and impurity heating are

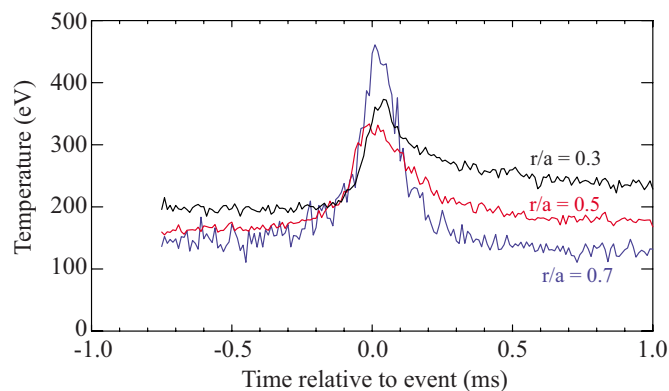


FIG. 11. (Color online) Ensemble-averaged measurements of the D^+ temperature from RS at three radial locations for a global reconnection event.

also taken into account, the fraction of converted energy would be somewhat higher. In the following section, we consider how the ion heating during global reconnection events relates to the change in magnetic energy for a range of plasma discharge conditions.

B. Variation of ion heating with plasma current and density

Measurements of the ion temperature evolution during a global reconnection event have been obtained for two values of plasma current (250 and 500 kA) and three ranges of electron density (~ 0.4 – 0.8 , 0.8 – 1.2 , and 1.2 – 1.8×10^{19} m^{-3}) using CHERS. Results were obtained at two plasma radii ($r/a=0$ and 0.55), and are shown in Figs. 12 and 13. In all cases, the results represent ensemble averages taken over many similar reconnection events, and error bars were estimated by assuming signal noise to be dominated by Poisson photon counting statistics. The temporal behavior of T_C is similar to that observed in Fig. 6, though these data are noisier because fewer events are included in the ensemble average. There are nonetheless a number of conclusions that can be drawn from looking at Figs. 12 and 13. First, the increase in T_C scales nonlinearly with plasma current, as the temperature more than doubles when I_p doubles. This is true both on-axis as well as at the mid-radius. At low plasma current, the variation of ΔT_C with density is fairly weak, whereas at high plasma current the variation of ΔT_C with density is also weak at $r/a=0$ but is significant at $r/a=0.55$. The results indicate that at high current, the ion temperature profile during reconnection becomes more peaked as the density increases. One possible explanation for this behavior is the presence of enhanced confinement periods during low density, high current operation, which could explain both the flat temperature profile observed during reconnection as well as the long tail observed in T_C after reconnection.

To develop a better understanding of the relative strength of the heating during reconnection, the total energy gained by the carbon ions for each of the scenarios shown in Figs. 12 and 13 is compared with the corresponding drop in stored magnetic energy. The former is calculated by assuming a “three-point” temperature model, using the measured values

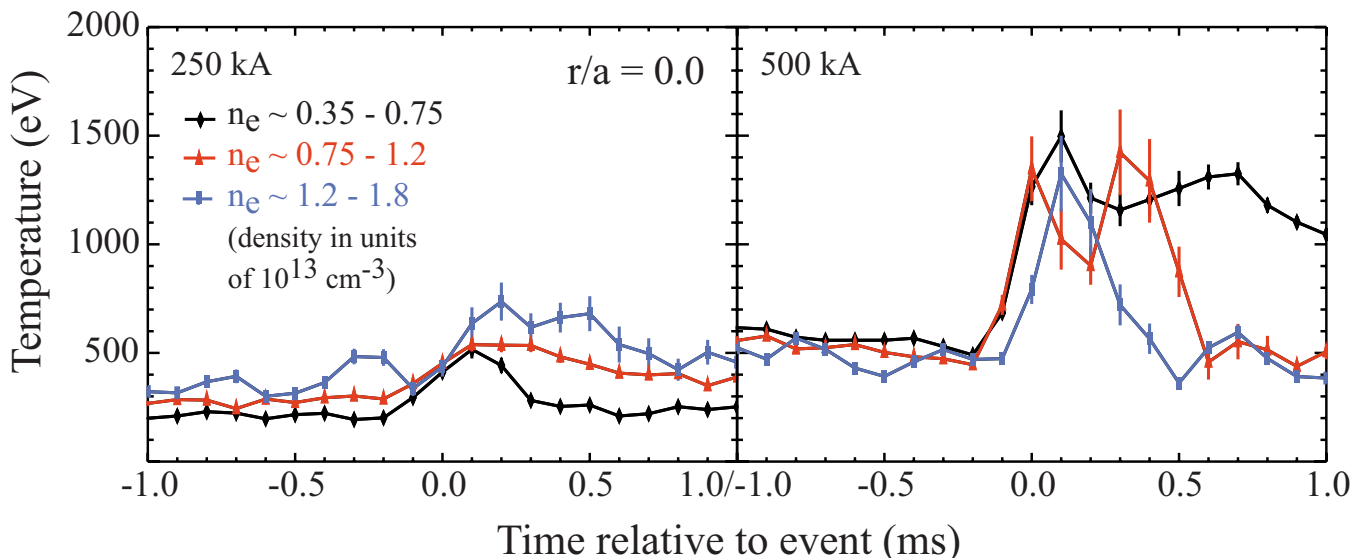


FIG. 12. (Color online) CHERS measurements of on-axis ($r/a=0$) ion heating during a global reconnection event for various plasma conditions. Left: Ensemble-averaged C^{+6} temperature data from three different density ranges at $I_p=250$ kA. Right: Ensemble-averaged C^{+6} temperature data from three different density ranges at $I_p=500$ kA.

for T_C at $r/a=0$ and 0.55 and assuming $T_C=0$ at $r/a=1$. The carbon density is assumed to be 1% of the electron density under all conditions (i.e., for all values of n_e and I_p), and this density is assumed not to change during the reconnection event. Although this assumption is not entirely valid, the change in density during the event is small compared to the change in temperature, so the assumption is expected to introduce little error into the calculation. Using this simple model, $\Delta U_{\text{thermal}}$ is calculated for each scenario, and then compared to $\Delta U_{\text{magnetic}}$, as shown in Table I.

There are a number of conclusions that can be drawn from these results. First, the fraction of the magnetic energy going into the carbon ions is small (under the assumption that the carbon density is 1% of n_e). However, as we saw in

Sec. V A, the majority ions are also significantly heated during reconnection, indicating that during reconnection, a substantial fraction of the stored magnetic energy goes into ion heating. At low plasma current, the change in ion thermal energy during reconnection scales strongly with density, even though the change in magnetic energy is independent of density. This result suggests that the heating per ion is equally efficient regardless of the ion density. This result does not appear to hold at high current, as the change in thermal energy drops off significantly with increasing density in this case. Under the assumptions of the model, this drop off is mostly accounted for by the small increase in T_C during reconnection at $r/a=0.55$. It is possible that at high current and high density, coupling between carbon and deute-

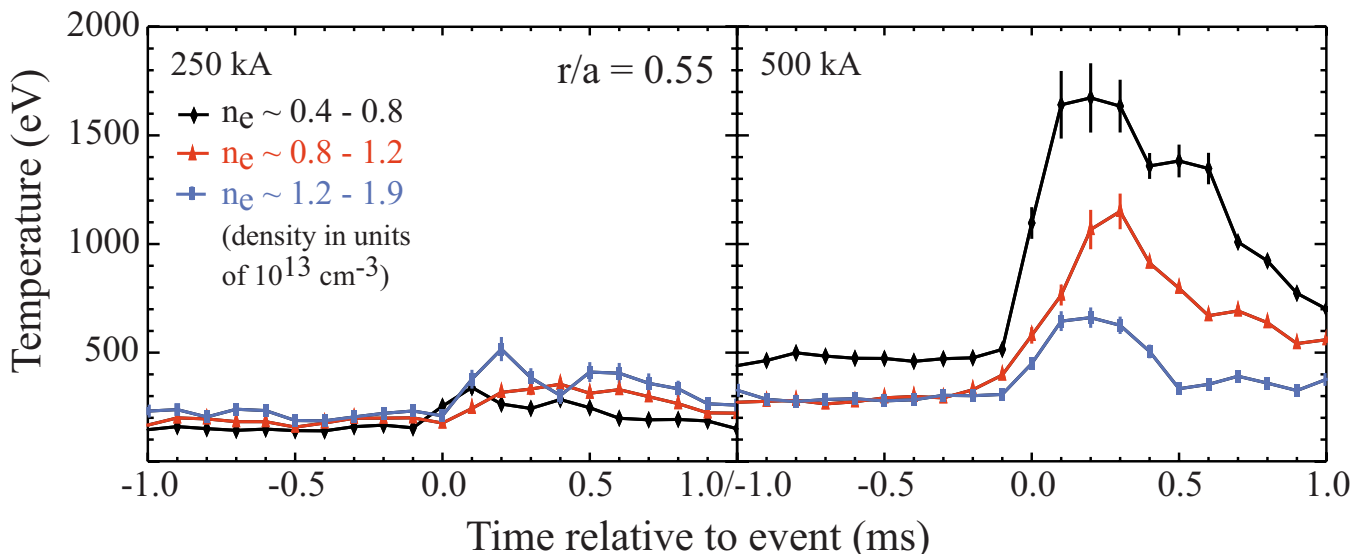


FIG. 13. (Color online) CHERS measurements of mid-radius ($r/a=0.55$) ion heating during a global reconnection event for various plasma conditions. Left: Ensemble-averaged C^{+6} temperature data from three different density ranges at $I_p=250$ kA. Right: Ensemble-averaged C^{+6} temperature data from three different density ranges at $I_p=500$ kA.

TABLE I. A comparison between the change in thermal energy and the change in stored magnetic energy for ensembles of global reconnection events generated at various plasma currents and densities.

I_p (kA)	$n_e(10^{19} \text{ m}^{-3})$	$\Delta U_{\text{thermal}}(\text{J})$	$\Delta U_{\text{magnetic}}(\text{J})$
250	0.35–0.75	10	6000
250	0.75–1.20	19	6000
250	1.20–1.80	43	5000–6000
500	0.40–0.80	76	28000–36000
500	0.80–1.20	99	28000
500	1.20–1.90	79	22000–24000

rium ions is strong enough that energy losses in the deuterium ion channel during reconnection (e.g., from charge-exchange losses, which would be stronger at the mid-radius relative to the plasma core) affect the carbon ion channel, resulting in a smaller increase in T_C . It is also possible that at high plasma current, the heating efficiency during reconnection is strongly reduced as the density is increased.

Perhaps the most interesting result is that during reconnection, the change in carbon thermal energy scales fairly well with the change in stored magnetic energy. For instance, at low current and low density $\Delta U_{\text{thermal}}/\Delta U_{\text{magnetic}} \sim 0.16\%$, while at high current and low density $\Delta U_{\text{thermal}}/\Delta U_{\text{magnetic}} \sim 0.24\%$ (the larger value at high current could again be the result of enhanced confinement periods present for high current, low density operation). Similarly, for low current and intermediate densities ($n_e = 0.75\text{--}1.20 \times 10^{19} \text{ m}^{-3}$) $\Delta U_{\text{thermal}}/\Delta U_{\text{magnetic}} \sim 0.32\%$, while for high current and intermediate densities $\Delta U_{\text{thermal}}/\Delta U_{\text{magnetic}} \sim 0.35\%$. These results suggest that the change in thermal energy during reconnection is directly connected to the drop in stored magnetic energy, indicating once again that the magnetic field is the energy source for ion heating during reconnection.

VI. POTENTIAL HEATING MECHANISMS

A number of mechanisms have been proposed to explain ion heating during magnetic reconnection. Localized, energetic outflows are produced as a result of reconnection, and collisional viscous damping of these flows could produce an increase in the ion thermal energy.^{31–33} Simulations indicate that on MST cross-field flows would have to be comparable to the thermal ion sound speed and vary strongly over a gyroradius scale for perpendicular viscosity to be effective in heating the ions.³⁴ Such large and localized flows have yet to be observed experimentally. Parallel viscosity is responsible for damping neoclassical parallel flows^{35,36} as well as cross-field compressional flows,^{31,33} and may therefore play an important role in transferring energy from tearing fluctuations to the ions, as the parallel viscosity coefficient is significantly larger than the perpendicular viscosity coefficient.³⁷ The effects of parallel viscosity in MST are currently being studied using calculated tearing mode flow profiles. Theoretical work is also being conducted to investigate the connection between ion heating and electron thermal transport.³⁸

Ion heating may also result from the turbulent cascade of tearing fluctuations to cyclotron frequencies.^{4,39} However, the role of cyclotron damping in heating ions during magnetic reconnection remains an open question, and is under theoretical investigation.⁴⁰ Previous measurements of the fluctuation power spectrum during global reconnection events in MST indicated energy loss at $\omega = \omega_{ci}$.⁴ However, ion heating by cyclotron waves is expected to be anisotropic, while no anisotropy was observed in previous line-integrated measurements of T_{\parallel} and T_{\perp} .⁶ As a result of MST's magnetic topology, current CHERS measurements yield a mix of both parallel (on-axis) and perpendicular (in the edge) ion temperature. Additional views are being designed to provide complete localized measurements of T_{\parallel} and T_{\perp} , so that the effects of cyclotron damping may be accurately assessed.

VII. SUMMARY

Spatially resolved measurements of the impurity ion temperature evolution during three types of impulsive reconnection event in MST have been obtained using charge-exchange recombination spectroscopy. Results indicate that the ion temperature increase is limited to the outer half of the plasma during an edge reconnection event, and that the heating is largest near the location of reconnection. Conversely, the ion temperature is observed to increase at all radial locations during a global reconnection event, indicating that heating occurs over a broad radial extent during such an event. Heating is also large in this case, causing the impurity ion temperature to increase by a factor of 2 or more. For both types of event, the drop in magnetic energy is sufficient to explain the increase in ion thermal energy. In addition, the time scale for heating in both cases is of order the reconnection time, indicating a large power flow into the ions during reconnection. The correspondence between the heating and reconnection locations and the heating and reconnection time scales implies that the observed heating is directly related to reconnection. However, not all impulsive reconnection events lead to ion heating. During a core reconnection event, the stored magnetic energy remains constant, as does the impurity ion temperature. A drop in stored magnetic energy is therefore required for ions to be heated during reconnection. When this occurs, heating is localized near the reconnection layer, as observed during an edge reconnection event. Consequently, the broad heating observed during a global reconnection event arises from the presence of reconnection activity at multiple resonant locations distributed throughout the plasma volume.

The magnitude and spatial structure of heating during a global reconnection event depend strongly on the background plasma current and density. Nonetheless, the change in the impurity ion thermal energy appears to scale linearly with the change in magnetic energy, offering more evidence for the direct relationship between ion heating and reconnection. Heating during a global reconnection event is stronger for impurities than for bulk ions in a deuterium background plasma, suggesting that the heating mechanism is ion-species-dependent. However, results obtained from helium background plasmas indicate similar heating between impu-

rities and the bulk. These results indicate that much more work is needed before we can understand the mechanisms responsible for heating ions during magnetic reconnection.

ACKNOWLEDGMENTS

This work was made possible by the excellent scientists, engineers, students, and technical staff on the MST team.

This work is supported by the U.S. Department of Energy and the National Science Foundation.

- ¹Y. Miura, F. Okano, N. Suzuki, M. Mori, K. Hoshino, T. Takizuka, K. Itoh, and S.-I. Itoh, *Phys. Plasmas* **3**, 3696 (1996).
- ²G. A. Wurden, P. G. Weber, K. F. Schoenberg *et al.*, in *Proceedings of the 15th European Conference on Controlled Fusion and Plasma Physics*, Dubrovnik, 1988 (Europhysics Conference Abstracts, Mulhouse, 1988), p. 533.
- ³A. Fujisawa, H. Ji, K. Yamagishi, S. Shinohara, H. Toyama, and K. Miyamoto, *Nucl. Fusion* **31**, 1443 (1991).
- ⁴E. Scime, S. Hokin, N. Mattor, and C. Watts, *Phys. Rev. Lett.* **68**, 2165 (1992).
- ⁵P. Horling, G. Hedin, J. H. Brzozowski, E. Tennfors, and S. Mazur, *Plasma Phys. Controlled Fusion* **38**, 1725 (1996).
- ⁶D. J. Den Hartog and D. Craig, *Plasma Phys. Controlled Fusion* **42**, L47 (2000).
- ⁷J. C. Fernandez, T. R. Jarboe, S. O. Knox, I. Henins, and G. J. Marklin, *Nucl. Fusion* **30**, 67 (1990).
- ⁸Y. Ono, M. Yamada, T. Akao, T. Tajima, and R. Matsumoto, *Phys. Rev. Lett.* **76**, 3328 (1996).
- ⁹A. Ejiri, S. Shiraiwa, Y. Takase *et al.*, *Nucl. Fusion* **43**, 547 (2003).
- ¹⁰R. G. O'Neill, A. J. Redd, W. T. Hamp, R. J. Smith, and T. R. Jarboe, *Phys. Plasmas* **12**, 122506 (2005).
- ¹¹E. R. Priest, C. R. Foley, J. Heyvaerts, T. D. Arber, J. L. Culhane, and L. W. Acton, *Nature* **393**, 545 (1998).
- ¹²P. A. Sturrock, *Astrophys. J.* **521**, 451 (1999).
- ¹³T. D. Phan, B. U. Sonnerup, and R. P. Lin, *J. Geophys. Res.* **106**, 25489, DOI: 10.1029/2001JA900054 (2001).
- ¹⁴E. R. Priest and T. G. Forbes, *Astron. Astrophys. Rev.* **10**, 313 (2002).
- ¹⁵A. Bhattacharjee, *Annu. Rev. Astron. Astrophys.* **42**, 365 (2004).
- ¹⁶R. J. Hastie, *Astrophys. Space Sci.* **256**, 177 (1997).
- ¹⁷R. G. Watt and R. A. Nebel, *Phys. Fluids* **26**, 1168 (1983).
- ¹⁸S. C. Hsu, G. Fiksel, T. A. Carter, H. Ji, R. M. Kulsrud, and M. Yamada, *Phys. Rev. Lett.* **84**, 3859 (2000).
- ¹⁹A. Stark, W. Fox, J. Egedal, O. Grulke, and T. Klinger, *Phys. Rev. Lett.* **95**, 235005 (2005).
- ²⁰R. N. Dexter, D. W. Kerst, T. W. Lovell, S. C. Prager, and J. C. Sprott, *Fusion Technol.* **19**, 131 (1991).
- ²¹H. P. Furth, *Phys. Fluids* **28**, 1595 (1985).
- ²²D. J. Den Hartog, D. Craig, D. A. Ennis *et al.*, *Rev. Sci. Instrum.* **77**, 10F122 (2006).
- ²³R. J. Fonck, R. J. Goldston, R. Kaita, and D. Post, *Appl. Phys. Lett.* **42**, 239 (1983).
- ²⁴R. C. Isler and L. E. Murray, *Appl. Phys. Lett.* **42**, 355 (1983).
- ²⁵D. Craig, D. J. Den Hartog, D. A. Ennis, S. Gangadhara, and D. Holly, *Rev. Sci. Instrum.* **78**, 013103 (2007).
- ²⁶S. Gangadhara, D. Craig, D. A. Ennis, and D. J. Den Hartog, *Rev. Sci. Instrum.* **77**, 10F109 (2006).
- ²⁷J. C. Reardon, G. Fiksel, C. B. Forest, A. F. Abdrashitov, V. I. Davydenko, A. A. Ivanov, S. A. Korepanov, S. V. Murachtin, and G. I. Shulzhenko, *Rev. Sci. Instrum.* **72**, 598 (2001).
- ²⁸S. Gangadhara, D. Craig, D. A. Ennis, D. J. Den Hartog, G. Fiksel, and S. C. Prager, *Phys. Rev. Lett.* **98**, 075001 (2007).
- ²⁹J. S. Sarff, S. A. Hokin, H. Ji, S. C. Prager, and C. R. Sovinec, *Phys. Rev. Lett.* **72**, 3670 (1994).
- ³⁰B. E. Chapman, C.-S. Chiang, S. C. Prager, J. S. Sarff, and M. R. Stoneking, *Phys. Rev. Lett.* **80**, 2137 (1998).
- ³¹C. G. Gimblett, *Europhys. Lett.* **11**, 541 (1990).
- ³²Z. Yoshida, *Nucl. Fusion* **31**, 386 (1991).
- ³³A. Ejiri and K. Miyamoto, *Plasma Phys. Controlled Fusion* **37**, 43 (1995).
- ³⁴V. A. Svidzinski, V. V. Mirnov, and S. C. Prager, *Bull. Am. Phys. Soc.* **50**, 37 (2005).
- ³⁵S. P. Hirshman and D. J. Sigmar, *Nucl. Fusion* **21**, 1079 (1981).
- ³⁶A. L. Garcia-Pericente, J. D. Callen, K. C. Shaing, and C. C. Hegna, *Phys. Plasmas* **12**, 052516 (2005).
- ³⁷S. I. Braginskii, *Rev. Plasma Phys.* **1**, 205 (1965).
- ³⁸R. Gatto and P. W. Terry, *Phys. Plasmas* **8**, 825 (2001).
- ³⁹N. Mattor, P. W. Terry, and S. C. Prager, *Comments Plasma Phys. Controlled Fusion* **15**, 65 (1992).
- ⁴⁰V. Tangri and P. W. Terry, *Bull. Am. Phys. Soc.* **51**, 75 (2006).